



ELSEVIER

Study of structural differences between stoichiometric and congruent lithium niobate

A. Kling^{a,*}, J.G. Marques^a, J.G. Correia^{a,d}, M.F. da Silva^b, E. Diéguez^c,
F. Agulló-López^c, J.C. Soares^a

^a Centro de Física Nuclear, Universidade de Lisboa, Av. Prof. Gama Pinto 2, P-1699 Lisboa, Portugal

^b Departamento de Física, ITN, P-2685 Sacavém, Portugal

^c Departamento de Materiales, C-IV, Universidad Autónoma, E-28049 Madrid, Spain

^d ISOLDE Collaboration, CERN, CH-1211 Genève, Switzerland

Abstract

The structural differences between stoichiometric and congruent (lithium deficient) lithium niobate single crystals were studied by RBS- and NRA-channeling as well as perturbed angular correlation (PAC) measurements. The ¹¹¹Cd-PAC investigations point out that a second Li site can be detected in congruent material, while only one is present in stoichiometric. Channeling studies of different axes and the comparison of the results with computer simulations corroborated former indications that this additional lattice site can be attributed to the formation of ilmenite type stacking faults. A comparative study of the energy dependence of the dechanneling showed that a remarkable disorder is also present in the Nb sublattice of the congruent crystals and that these defects have a point-like character.

1. Introduction

Although lithium niobate (LiNbO₃) has a wide range of applications, some of its basic structural properties are still the subject of intense discussions. For crystals grown from a congruently melting composition with a Li to Nb ratio of [Li]/[Nb] = 0.945 the decision is still to be made between three main defect models: the lithium vacancy model [1], the Nb vacancy model [2] and the stacking fault model [3]. Computer simulations pointed out that the formation of ilmenite-type stacking sequences is likely to occur in congruent lithium niobate due to energetic reasons [4].

Comparative investigations of congruent and stoichiometric material, became practical with the recent growth of bulk stoichiometric crystal. A previous study revealed that two non-equivalent Li sites exist in congruent LiNbO₃ and cause structural disorder in the lithium sublattice [5]. Angular scans with RBS-NRA-channeling for the (0001) plane and the $\langle 11\bar{2}0 \rangle$ axis yielded results compatible with the occurrence of ilmenite type stacking faults. However, no information about disorder in the Nb sublattice and the size of the defects could be obtained.

In order to address these questions, results on the energy dependence of the dechanneling are presented in this work. Also, additional RBS-NRA-channeling and PAC stud-

ies, which strengthen our previous conclusions, were carried out.

2. Experimental details

LiNbO₃ crystals with a composition close to stoichiometry [Li]/[Nb] = 0.979 [5] were grown in Madrid by the Czochralski method, while congruent crystals were obtained from Munich and Budapest.

The ion beam experiments were performed at the 3.1 MeV Van de Graaff accelerator at Sacavém, using a 1.6 MeV proton beam for the angular scans. This enabled simultaneous recording of Nb-RBS and Li-NRA (using the ⁷Li(p,α)⁴He reaction) spectra. For the measurements of the energy dependence of the dechanneling, spectra were recorded for proton beams with energies ranging from 0.75 to 1.75 MeV increasing in steps of 0.25 MeV. To minimize the influence of dechanneling due to radiation damage induced by the analyzing beam, each measurement was performed on a virgin spot of the sample. The difference in the minimum yields $\Delta\chi_{\min}$ at a fixed depth interval yields information about the type and size of defects in a non-perfect crystal [7]. For point defects an energy dependence $\sim E^{-\kappa}$ is observed, with κ ranging from unity for isolated point defects, to 0.50 for larger defect clusters. In contrast, for extended defects which act like internal “surfaces”, $\Delta\chi_{\min}$ is a constant. To take into account both cases in this work the fits were performed with

* Corresponding author.

the function

$$\delta + cE^{-\kappa}. \quad (1)$$

For the PAC measurements, radioactive ^{111m}Cd was implanted at 60 keV into stoichiometric LiNbO_3 crystals, at a dose of $5 \times 10^{12} \text{ cm}^{-2}$, using the ISOLDE/CERN isotope separator. For a projected range of 23 nm, calculated by TRIM, a maximum concentration of $1 \times 10^{18} \text{ Cd at/cm}^3$ corresponding to 0.02 at% was derived. The samples were annealed at 600°C in air for 30 min. The well-known 151–245 keV cascade in the decay of ^{111m}Cd was used in the $e^- - \gamma$ PAC studies. Details on the experimental setup [6] and the evaluation of ^{111m}Cd PAC measurements [5] can be found elsewhere. Two different geometries were used, with the c -axis and the detector's plane forming different angles in order to determine the asymmetry parameter η unambiguously.

3. Results and discussion

A comparison of Nb-RBS and Li-NRA angular scans along the $\langle 01\bar{1}0 \rangle$, $\langle 02\bar{2}1 \rangle$ and $\langle 0\bar{4}41 \rangle$ axes obtained in congruent and stoichiometric samples is shown in Fig. 1. The experimental values for the Nb-RBS scans, at a depth interval ranging from the surface to 4500 Å, exhibit no significant differences between the two types of samples. For

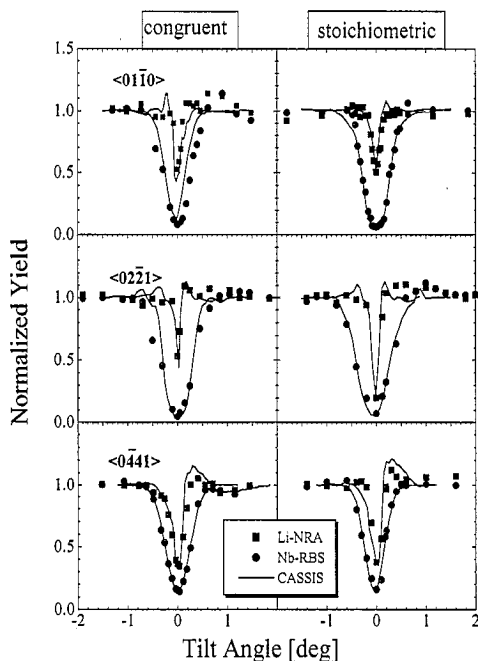


Fig. 1. Comparison of the Nb-RBS and Li-NRA angular scans of congruent and stoichiometric LiNbO_3 for (a) $\langle 01\bar{1}0 \rangle$, (b) $\langle 02\bar{2}1 \rangle$ and (c) $\langle 0\bar{4}41 \rangle$ axis. The solid lines are computer simulations using CASSIS for a congruent crystal containing 2% dilute ilmenite type stacking sequences and for a stoichiometric one, respectively.

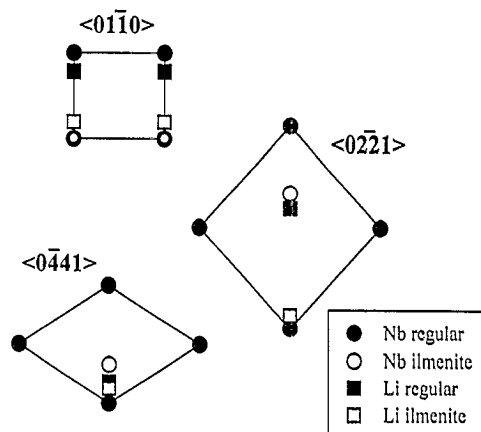


Fig. 2. Projections of the $\langle 01\bar{1}0 \rangle$, $\langle 02\bar{2}1 \rangle$ and $\langle 0\bar{4}41 \rangle$ axes of lithium niobate showing the regular cation sites (solid symbols) and additional cation sites introduced by ilmenite stacking faults (open symbols).

all defect models the fraction of displaced niobium atoms is low, so that only a small influence on the minimum yield in the investigated depth interval is expected. Also the Li-NRA angular scans for the $\langle 01\bar{1}0 \rangle$ and $\langle 0\bar{4}41 \rangle$ axes are similar for congruent and stoichiometric samples. As depicted in Fig. 2 the additional Li- and Nb-lattice sites due to ilmenite type stacking faults are located close to the regular positions of the LiNbO_3 lattice. Therefore no major influence on the Li-NRA χ_{\min} is expected in these axes. In the case of the $\langle 02\bar{2}1 \rangle$ axis the additional Nb lattice site is located close to the center of the channel. Due to the almost central position of the regular Li site, the Li-NRA angular scan is very narrow compared to the Nb-RBS, and even a small amount of defects will enhance the probability for a lithium nuclear reaction, causing an increase of the Li-NRA χ_{\min} .

The solid lines show the results of calculation with the channeling Monte Carlo simulation code CASSIS [8], assuming a perfect LiNbO_3 lattice for the stoichiometric and a lattice with 2% dilute stacking fault sequences of the ilmenite type for the congruent crystal. The simulations fit the experimental data very well.

Fig. 3 shows the minimum yields obtained for the $\langle 11\bar{2}0 \rangle$, $\langle 01\bar{1}0 \rangle$ and $\langle 02\bar{2}1 \rangle$ axes for a depth interval from 1.0 to 1.5 μm , as a function of the energy of the incident protons, for a) congruent and b) stoichiometric single crystals. The χ_{\min} values for the congruent case are significantly higher than those for the stoichiometric, pointing to a remarkable dechanneling due to defects in the Nb sublattice of the congruent material.

Based on previous results, the lattice of stoichiometric LiNbO_3 can be regarded as perfect [5] and therefore the difference of the minimum yields between congruent and stoichiometric crystal $\Delta\chi_{\min}$, plotted in Fig. 3c, serves as a measure for the dominant defects in the congruent sample. Fitting a function of the type given in equation (1) yields $\delta = -0.015, 0.000, -0.031$ and $\kappa = 0.67, 0.70, 0.79$ for

$\langle 11\bar{2}0 \rangle$, $\langle 01\bar{1}0 \rangle$ and $\langle 02\bar{2}1 \rangle$, respectively. The values for δ , which are zero or negative exclude the existence of extended defects, such as microcrystalline inclusions with different lattice structure or ferroelectric micro domains in the congruent sample. On the other hand, the values for κ are close to the theoretical limit of $\kappa = 1$ for isolated defects, limiting the size of stacking fault sequences to a few lattice constants and require a dilute distribution in the crystal.

Fig. 4 shows the PAC spectra obtained for the near-stoichiometric sample for the two geometries, which are well described by one frequency $\nu_Q = 191(2)$ MHz and a null asymmetry parameter $\eta = 0$. In contrast, in congruent samples two close frequencies, $\nu_Q(I) = 191(2)$ MHz and $\nu_Q(II) = 205(2)$ MHz, with non-zero η [9] had to be considered. From the channeling results in this work, these two frequencies can be assigned to ^{111}Cd probes occupying two distinct Li sites in the congruent crystals. The null asymmetry parameter obtained in the stoichiometric sample indicate a higher lattice perfection of this crystal.

4. Conclusions

Investigations using ion beam analysis and hyperfine interaction techniques confirmed and furthered previous results on both the perfection of the lattice in stoichiometric LiNbO_3 and on disorder in the lithium sublattice of congruent LiNbO_3 . The two distinct lithium lattice sites in the congruent samples found in investigations by PAC can be,

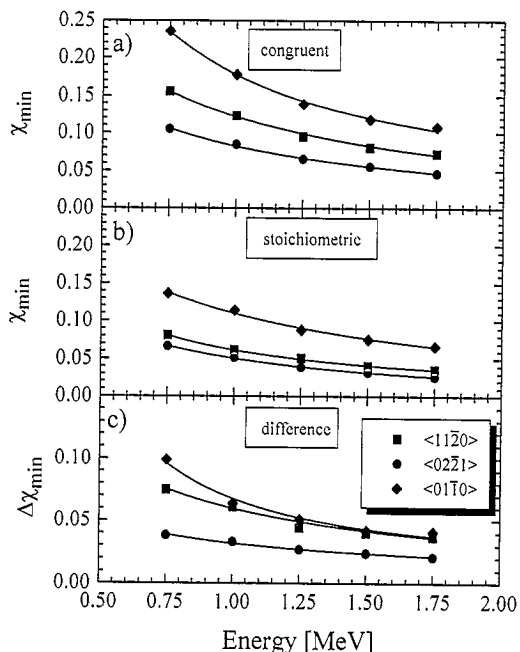


Fig. 3. Energy dependence of the dechanneling of protons in (a) congruent and (b) stoichiometric LiNbO_3 for the $\langle 11\bar{2}0 \rangle$, $\langle 01\bar{1}0 \rangle$ and $\langle 02\bar{2}1 \rangle$ axes. c) The difference $\Delta\chi_{\min}$ can be fitted by functions of the type $E^{-\kappa}$ with κ between 0.69 and 0.78 in accordance with pointlike defects.

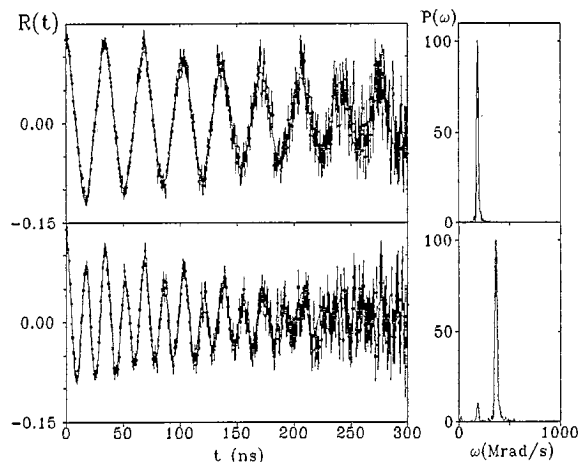


Fig. 4. Time dependent anisotropy of the 151–245 keV $e^- - \gamma$ cascade of ^{111}Cd in near-stoichiometric LiNbO_3 , with c-axis perpendicular to the detectors' plane (top), and c-axis in the detectors' plane at 45° with two detectors (bottom).

according to the results of the angular scans of Li-NRA and their modeling by computer simulations, attributed to the occurrence of short stacking fault sequences of the ilmenite type. From the calculations a fraction of 2% stacking faults in the congruent crystal is derived. The comparative study of the energy dependence of dechanneling between congruent and stoichiometric samples proved the existence of point-like structural disorder in the niobium sublattice. A substantial influence of extended defects like ferroelectric micro domains on the defect structure can be definitely excluded.

Acknowledgements

This work has been supported by JNICT, Portugal, through CERN project 137/94, and a PhD grant (J.G.M.).

References

- [1] P. Lerner, C. Legras, J.P. Dumas, *J. Cryst. Growth* 3/4 (1968) 231.
- [2] S.C. Abrahams, P. Marsh, *Acta Crystallogr. B* 42 (1986) 61.
- [3] K. Nassau, M.E. Lines, *J. Appl. Phys.* 41 (1970) 533.
- [4] H. Donnerberg, S.M. Tomlinson, C.R.A. Catlow, O.F. Schirmer, *Phys. Rev. B* 40 (1989) 11909.
- [5] A. Kling, L. Rebouta, J.G. Marques, J.G. Correia, M.F. da Silva, E. Diéguez, F. Agulló-López, J.C. Soares, accepted for publication in *Nucl. Instr. and Meth. B*.
- [6] J.G. Marques, J.G. Correia, A.A. Melo, M.F. da Silva, J.C. Soares, ISOLDE Collaboration, *Nucl. Instr. Meth. B* 99 (1995) 645.
- [7] K. Gärtner, K. Hehl, G. Schlotzhauer, *Nucl. Instr. Meth. B* 4 (1984) 55.
- [8] A. Kling, *Nucl. Instr. Meth. B* 102 (1995) 141.
- [9] B. Hauer, R. Vianden, J.G. Marques, N.P. Barradas, J.G. Correia, A.A. Melo, J.C. Soares, F. Agulló-López, E. Diéguez, *Phys. Rev. B* 51 (1995) 6208.